

Improved tetrahedron method for Brillouin-zone integrations

Peter E. Blöchl*

IBM Research Division, Zurich Research Laboratory, CH-8803 Rüschlikon, Switzerland

O. Jepsen and O. K. Andersen

Max-Planck-Institut FKF, Heisenbergstrasse 1, D-70569 Stuttgart, Germany

(Received 29 October 1993)

Several improvements of the tetrahedron method for Brillouin-zone integrations are presented. (1) A translational grid of k points and tetrahedra is suggested that renders the results for insulators identical to those obtained with special-point methods with the same number of k points. (2) A simple correction formula goes beyond the linear approximation of matrix elements within the tetrahedra and also improves the results for metals significantly. For a required accuracy this reduces the number of k points by orders of magnitude. (3) Irreducible k points and tetrahedra are selected by a fully automated procedure, requiring as input only the space-group operations. (4) The integration is formulated as a weighted sum over irreducible k points with integration weights calculated using the tetrahedron method once for a given band structure. This allows an efficient use of the tetrahedron method also in plane-wave-based electronic-structure methods.

I. INTRODUCTION

The translational symmetry of solids results in a quantum number, namely, the crystal momentum \vec{k} . Band-structure calculations exploit this symmetry to block-diagonalize the Hamiltonian. Consequently all one-particle expectation values are represented as an integral of the matrix elements over the Brillouin zone or the occupied regions thereof. The accuracy and the computational effort of electronic-structure calculations for solids depends directly on these Brillouin-zone integrations, because they determine how many k points have to be considered for a given accuracy.

For performing Brillouin-zone integrations, the following two methods are most widely used: the tetrahedron method^{1,2} and the special-point scheme.^{3,4} The special-point scheme is limited to insulating or semiconducting materials, and represents the Brillouin-zone integration as a weighted sum over selected k points. Today, the most widely used sets of special points are those of Monkhorst and Pack,⁵ which consist of an equispaced grid of k points. A more general integration scheme is the tetrahedron method, which is equally applicable to insulators and metals. Here, reciprocal space is divided into tetrahedra, within which matrix elements and band energies are linearized in \vec{k} . The linear approximation allows the integration to be performed analytically, taking into account the often complicated shape of the Fermi surface. In addition, the tetrahedron method is superior to the special-point method in providing spectral functions.

Even though the tetrahedron method is generally applicable, it has a number of shortcomings in its usual application, which consists in dividing the irreducible part

of the Brillouin zone into tetrahedra. For insulators, the number of k points required for a given accuracy is substantially larger than that of the special-point method. Dividing the irreducible part of the first Brillouin zone for each symmetry group into tetrahedra is cumbersome. Performing the Brillouin-zone integration requires a large number of matrix elements to be available at the same time, an almost impossible task for any plane-wave-based electronic-structure program.

We show here that all these problems can easily be circumvented in a simple manner. By avoiding the misweighting problem discussed earlier,^{6,7} we obtain results for insulators that are identical to those of the Monkhorst and Pack special-point method.⁵ For metals, however, avoiding misweighting alone only improves the results marginally. An analysis of the errors led us to a correction formula that improves the accuracy of the tetrahedron method by taking into account the curvature of the integrand. As a result we obtain an easy-to-use tetrahedron method that provides the same accuracy as the special-point method for semiconductors. Also for metals the new method is far superior to the previous tetrahedron method and results in typical savings of computational time by factors of 10–100 in electronic-structure calculations. The method described here was developed earlier,⁸ and has been used in several applications.⁹

In Sec. II we give a brief overview of the method and describe the main principles of our approach. Sections III–V provide an explicit description of the method. In Sec. III we describe our choice of k points and tetrahedra, and an automated procedure to generate irreducible k points and inequivalent tetrahedra. Our particular choice of tetrahedra is important for the use of the correction formula. Section IV describes how the tetrahedron in-

tegration is converted into a simple sum of the matrix elements at the irreducible k points, with integration weights calculated using the tetrahedron method. Section V discusses the convergence properties of the tetrahedron method and contains a derivation of the correction formula. In the last section, Sec. VI, we describe possible extensions and the relationship to other common approaches to Brillouin-zone integrations.

II. OVERVIEW

In a crystalline solid the lattice translation symmetry results in a quantum number, namely, the crystal momentum. Wave functions $\Psi_n(\vec{k})$ and eigenvalues $\epsilon_n(\vec{k})$ therefore depend on a band index n and the crystal momentum or k point \vec{k} . The expectation value $\langle X \rangle$ of an operator X is obtained by integrating the matrix elements

$$X_n(\vec{k}) = \langle \Psi_n(\vec{k}) | X | \Psi_n(\vec{k}) \rangle \quad (1)$$

over all occupied bands in reciprocal space

$$\langle X \rangle = \frac{1}{V_G} \sum_n \int_{V_G} d^3k X_n(\vec{k}) f(\epsilon_n(\vec{k})), \quad (2)$$

where V_G is the volume of the reciprocal unit cell and $f(\epsilon)$ is the occupation number. Here, we consider only the Fermi distribution function at zero temperature, which is equal to 1 for $\epsilon < \epsilon_F$ and zero for $\epsilon > \epsilon_F$. Finite-temperature results can be obtained as an energy integral over the zero-temperature results for various Fermi energies, weighted with the energy derivative of the finite-temperature Fermi distribution function multiplied by -1 .

In band-structure calculations, wave functions are calculated only for a finite set of k points, while the remaining values are recovered by interpolation. The ultimate goal of any Brillouin-zone method is to obtain accurate expectation values with a minimum number of k points for which the matrix elements have to be calculated explicitly. Symmetry is exploited to reduce the number of independent k points further.

In the traditional implementation of the tetrahedron method the irreducible part of the Brillouin zone is determined and divided into tetrahedra. Eigenvalues and matrix elements are obtained for the k points at the corners of the tetrahedra. Finally the integration for each tetrahedron is performed analytically, after linearly interpolating eigenvalues and matrix elements inside the tetrahedron. The details of the method are described elsewhere.^{1,2}

An analysis of the convergence behavior with increasing number of k points reveals that in general the integration error $\delta\langle X \rangle$ decreases as $\delta\langle X \rangle \propto \Delta^2$, where Δ is a characteristic spacing between k points. The number of k points that have to be considered is proportional to $1/\Delta^3$. The integration error can be decomposed into two terms. One is the integration error due to piecewise linear interpolation within the polyhedron that replaces

the Fermi surface. The other is the integral between the true Fermi surface and the polyhedron approximating it. In principle, both errors converge as Δ^2 . For the sum of one-electron energies and the total energy, however, the Fermi surface term only contributes errors of order Δ^4 , because both are variational with respect to changes of the Fermi surface. Hence the dominant error in total energy calculations stems from the integral within the polyhedron.

The error from the integration within the polyhedron is related to the overestimate of $X_n(\vec{k})$ for positive curvature of $X_n(\vec{k})$ and to the underestimate for negative curvature, as illustrated in Fig. 1. As will be shown below, the error can be related in leading order to an integral of the curvature of $X_n(\vec{k})$ over the occupied regions of k space. This integral can be transformed via the Gauss theorem into an integral involving only first derivatives of $X_n(\vec{k})$ over the surface enclosing the integration region. The resulting surface integral can be evaluated, because the first derivatives of the matrix elements are readily accessible within the tetrahedron method.

With a particular arrangement of the tetrahedra, based on an equispaced grid of k points and a translationally symmetric arrangement of tetrahedra described below, this integral is an integral over the Fermi surface and the expressions are independent of the coordinates of the k -point positions, which is also the case for the original formulation of the tetrahedron method.

The correction formula evaluates the difference $\delta\langle X \rangle = \langle X \rangle - \langle \bar{X} \rangle$ between the integral of the true function $X(\vec{k})$ and the integral of its linearized version $\bar{X}(\vec{k})$ to leading order. It is given by

$$\delta\langle X \rangle = \sum_T \frac{D_T(\epsilon_F)}{40} \sum_{ij} \left(\epsilon_i X_j - \delta_{ij} \sum_m \epsilon_m X_m \right). \quad (3)$$

The outermost sum is a sum over all tetrahedra, $D_T(\epsilon_F)$ is the contribution of one tetrahedron to the density of states at the Fermi level, ϵ_i are the one-particle energies, and X_i are the matrix elements at the four corners of the tetrahedron. The k point index should not be confused with the band index, which is suppressed.

For insulators and semiconductors, the Fermi surface and consequently the correction term vanish. As will be described below we use an arrangement of tetrahedra

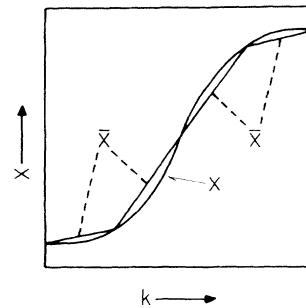


FIG. 1. Schematic representation of the interpolation error due to linear interpolation. Linearly interpolated matrix elements are indicated by \bar{X} .

that avoids misweighting of k points. In this case, it was shown earlier^{6,7} that the tetrahedron method maps identically onto the special-point scheme of Monkhorst and Pack.⁵ With the conventional choice of tetrahedra, the error decays very slowly even for insulators, namely, proportionally to Δ^2 , as shown in Fig. 2. With the new method, on the other hand, the integration error decays much more rapidly, namely, exponentially with Δ . This rapid convergence—faster than any power of the grid spacing—follows from the derivation of the special-point scheme from a Fourier interpolation of the matrix elements in k space.

For metals a simple rearrangement of the tetrahedra is not sufficient to improve convergence. However, the gain in accuracy by using the correction formula is substantial as illustrated for Cu and NiSi₂ in Figs. 3 and 4. With the new method, the convergence for metals is roughly comparable to that of the special-point method for insulators. The number of k points can be typically reduced by one or two orders of magnitude. The correction formula always improved the result, even for pathologically coarse submeshes. For increasingly finer meshes, the use of the correction formula rapidly becomes even more favorable.

We have also implemented two technical improvements that make the method substantially more versatile and easier to use, in addition to the increase in accuracy it offers. One shortcoming of previous implementations of the tetrahedron method was that the matrix elements of a large number of irreducible k points had to be accessible at the same time during integration. In plane-wave-based methods the charge density has to be integrated, which results in enormous amounts of data, if, for example, the full charge density of each band and k point needs to be available simultaneously. Therefore, a method that accumulates the matrix elements in a simple sum over bands and k points is highly desirable. This is the case in the special-point method, while in the traditional tetrahedron method the sum runs over tetrahedra, so that the same k point is used several times. We show here that the tetrahedron method can be expressed, even for metals, as

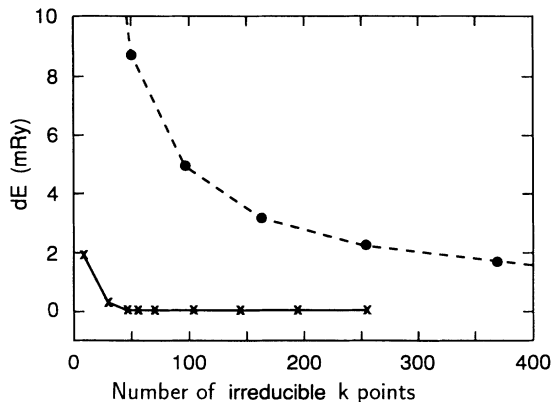


FIG. 2. Convergence of the band-structure energy of silicon (per atom) using our and the conventional tetrahedron method. Results with the new method are identical to the special-point scheme of Monkhorst and Pack. Submesh includes Γ point in this case. Lines are guides to the eye.

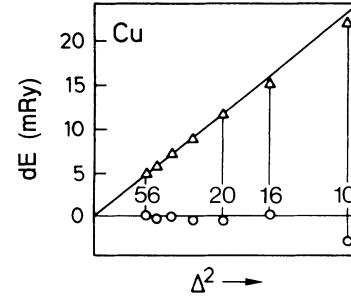


FIG. 3. Convergence of the band-structure energy of copper using our and the conventional tetrahedron method. Δ is the characteristic spacing between k points on the submesh in arbitrary units. Numbers indicate the number of irreducible k points.

a weighted sum over irreducible k points \vec{k}_j

$$\langle X \rangle = \sum_{j,n} X_n(\vec{k}_j) w_{nj}, \quad (4)$$

where the weights w_{nj} are independent of the matrix elements $X_n(\vec{k})$ and are calculated only once for a given set of energy bands with the tetrahedron method. Similar weights can be obtained for the evaluation of the density of states at a given energy. They are obtained as the energy derivatives of weights w_{nj} described above. Such a transformation of the integration into a weighted sum has independently been developed by Temmerman *et al.*¹⁰

There is a more general, underlying reason for the existence of a sampling formula such as Eq. (4): The integral is a linear functional and depends only on the matrix elements at a finite set of irreducible k points. Hence, the most general form of the integral is a sampling formula with the weights given by $w_{nj} = d\langle X \rangle / dX_n(\vec{k}_j)$. Because interpolation (also with nonlinear functions) and integration are linear operations, the integration weights are independent of the values of the matrix elements to be integrated. This implies that any integration scheme based on interpolation of the matrix elements between a finite set of k points can be expressed in exactly the same way.

The last point discussed in this paper is an automatic procedure for dividing space into tetrahedra and

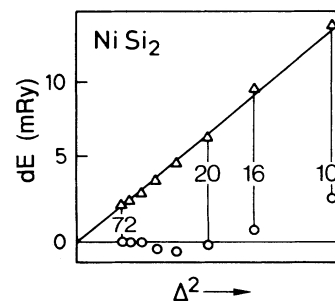


FIG. 4. Convergence of the band-structure energy of NiSi₂, as an example of a more complicated band structure, using the present and the conventional tetrahedron methods. Description as in Fig. 3.

for searching irreducible k points and tetrahedra for a given space-group symmetry. In the traditional implementations, the irreducible zone was first determined and then divided “by hand” into tetrahedra. This procedure is cumbersome, error prone because very complicated, and often results in a nonoptimum choice of tetrahedra. We will describe how the corresponding operations can easily be automated and performed by the computer “on the fly.” We first define a submesh of k points with equispaced grid points, and transform the submesh onto itself using the space-group operations to select irreducible points. Similarly, all tetrahedra in the unit cell are selected and subsequently reduced to an inequivalent set using a pointer array that points from every k point on the submesh to the corresponding irreducible k point. Since the choice of tetrahedra and k points is now largely independent of the point-group symmetry, near-optimum shapes for the tetrahedra can be selected.

III. SELECTION OF k POINTS AND TETRAHEDRA

First we define an equispaced grid in reciprocal space. The lattice vectors of the submesh are obtained by dividing a set of primitive reciprocal lattice vectors by the integers n_1 , n_2 and n_3 . Under the symmetry operations of the reciprocal lattice, the submesh should transform onto itself. This requires that the number of divisions along pairs of lattice vectors that are not parallel to either a three-, four-, or sixfold rotation axis must be equal. If one chooses to violate this condition, the corresponding symmetry operations must be excluded in the subsequent symmetry considerations. In many cases it is advisable to shift the grid by one-half of one or more lattice translation vectors of the submesh in order to avoid high-symmetry points. However, there is a trade-off, since in some cases such a shift reduces the number of point-group operations that can be exploited, because only symmetry operations that are shared between the reciprocal lattice of the solid and the submesh can be used.

Symmetry is used to identify a set of irreducible k points: Each k point is represented by a three-dimensional integer vector (i, j, k) . The elements of this vector correspond to twice the number of submesh translations from the Γ point, or a point that is offset from the Γ point by one submesh translation in one or several directions. The factor 2 is chosen so that shifted submeshes can also be handled. In this basis, each point-group operation can be represented by an *integer* 3×3 matrix. A subsequent reciprocal lattice vector transforms the result of a point-group operation applied to the integer vector (i, j, k) back into the first unit cell.

In order to simplify the comparison of k points, each submesh point in the first reciprocal unit cell or the corresponding shifted unit cell is given a unique number

$$N = 1 + \frac{i - i_0}{2} + (n_1 + 1) \left(\frac{j - j_0}{2} + (n_2 + 1) \frac{k - k_0}{2} \right). \quad (5)$$

The vector (i_0, j_0, k_0) describes the submesh shift. Its elements are zero except for the shift directions, for which they are 1. k points with positions characterized by $i_1/2 \in \{0, \dots, n_1\}$, $j/2 \in \{0, \dots, n_2\}$, and $k/2 \in \{0, \dots, n_3\}$ are included, so that k points on the boundaries of the unit cell are also considered. This would not be necessary for the search of irreducible k points in itself, but a full translational cell will later be divided into tetrahedra, which is facilitated if all surface points of a translational cell have also been included.

To find the irreducible points, we set up an integer pointer array indexed by the numbers of the k points according to Eq. (5) and initialized by the same numbers. Now we generate the submesh translations $(i + i_0)/2, (j + j_0)/2, (k + k_0)/2$ for each k point starting with the k point characterized by the smallest number according to Eq. (5). Each k point is successively transformed by all point-group operations and translated back into the first unit cell by a reciprocal lattice vector. If the resulting k point is characterized by a number smaller than the one stored in the pointer array, we replace that value by the pointer value for the newly created k point. In this case it is not necessary to apply the remaining point-group operations and we immediately proceed to the k point which is characterized by the next larger number according to Eq. (5). After this procedure has been applied to all k points, the array relates all submesh points to an irreducible set of k points. The irreducible points are isolated (value and index are identical for irreducible k points), and their coordinates are stored for use in the band-structure calculation. Each irreducible k point now receives a new number, referring to the order in which the coordinates of the irreducible k points are stored, and the pointer array is changed accordingly.

The next step defines the tetrahedra. Each submesh cell is divided into six tetrahedra of equal volume. As illustrated in Fig. 5 we choose one main diagonal of a

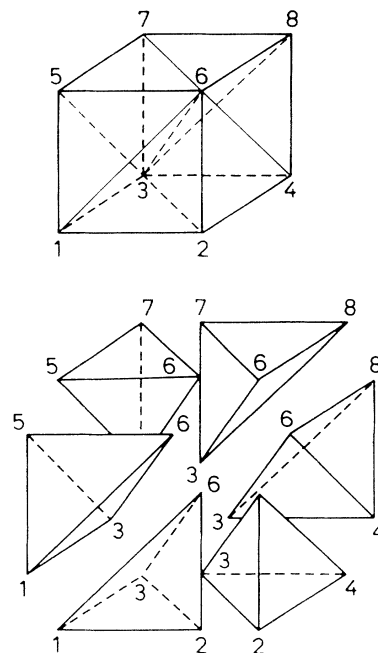


FIG. 5. Breakup of a submesh cell into six tetrahedra.

submesh cell as common edge of all six tetrahedra. In order to minimize interpolation distances the shortest main diagonal is chosen. Each tetrahedron is then identified by a quadruple of numbers, namely, the irreducible k -point labels in the pointer array corresponding to the four corners. The quadruples are then compared in order to obtain an irreducible set of tetrahedra and their multiplicities. The order of the k points within one quadruple is irrelevant and hence they are best ordered in a specific way, for example, such that irreducible k points with a smaller number precede those with a larger number. A possible practical approach is to map each quadruple in a unique way onto integers and use a standard ordering routine. (Note, however, that the number of digits of an integer is limited on a computer.)

The information about the tetrahedra, namely, the irreducible k points corresponding to the corners of the tetrahedra and the multiplicity of the inequivalent tetrahedra, is then stored for later use in the integration. In addition, the volume fraction of the reciprocal unit cell occupied by one tetrahedron is stored. Note that all tetrahedra have the same volume. All this information needs to be calculated only once for a given space-group symmetry.

Our procedure completely avoids the determination of an irreducible zone. Instead we discretize the problem from the outset, and perform the symmetry operations on the grid, which can be done efficiently and in a fully automated way on a computer. The only ingredients required are the point-group operations of the space group, which are listed, for example, in Bradley and Cracknell.¹¹ The full point group can also easily be constructed from a small number of generators of a point group.

IV. CONVERSION OF THE INTEGRAL INTO A WEIGHTED SUM

Here we describe how the integral can be transformed into a weighted sum, shown in Eq. (4), of the matrix elements at the irreducible k points with weights that are calculated by the tetrahedron method. This expression has the same structure as that of the special-point method, except that here the weights also depend on a band index. The weights are independent of the function to be integrated, and they are calculated only once for a given set of one-particle energies.

Any function $\bar{X}_n(\vec{k})$ that is obtained by linearly interpolating the function $X_n(\vec{k})$ within the tetrahedra can be written as a superposition of functions $w_j(\vec{k})$,

$$\bar{X}_n(\vec{k}) = \sum_j X_n(\vec{k}_j) w_j(\vec{k}), \quad (6)$$

where $w_j(\vec{k})$ is equal to 1 at the irreducible k point \vec{k}_j and its corresponding star, and zero at all other k points on the grid. (A star is the set of k points that can be transformed into a single k point with the space-group operations.) Within each tetrahedron $w_j(\vec{k})$ is a linear function. Such a function is shown schematically in Fig. 6. Every function $w_j(\vec{k})$ can now be integrated indepen-

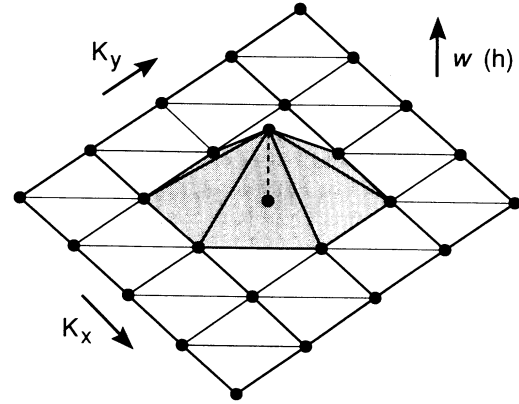


FIG. 6. Two-dimensional, schematic illustration of the functions $w_j(\vec{k})$ that result in the integration weights when integrated.

dently using the tetrahedron method.

Brillouin-zone integration of Eq. (6) results in Eq. (4) with the integration weights w_{nj} defined as

$$w_{nj} = \frac{1}{V_G} \int_{V_G} d^3k w_j(\vec{k}) f(\epsilon_n(\vec{k})). \quad (7)$$

In order to obtain the integration weights, one first has to find the position of the Fermi level. This may be obtained by calculating the total integrated density of states on an energy mesh covering possible Fermi level positions, which is then iteratively refined until the Fermi level is determined to a specified accuracy in the number of electrons. (A narrow energy range containing the Fermi level is easily obtained from the extrema of each band and the number of electrons.) The expressions needed to evaluate the integrated density of states are given in Appendix A.

The Fermi energy obtained in this way converges to the true Fermi energy as Δ^2 . It is important not to correct for this deviation in the expressions given below, because that would result in large errors for the expectation values, in particular for the number of electrons.

Once the Fermi level has been determined we can directly integrate the functions $w_j(\vec{k})$ over the occupied regions of k space to obtain the weights w_{nj} . The expressions for the integration weights are given in Appendix B.

For all fully occupied bands, the resulting weights are identical to the geometric factor used in the special-point method.

V. CORRECTION FORMULA

This section is devoted to an analysis of the integration errors of the tetrahedron method. The result of this discussion will be an extremely simple formula that corrects for most of the integration errors.

The dominant source of error in the tetrahedron method is the linear interpolation of the matrix elements inside each tetrahedron. This is shown schematically in

Fig. 1. If the curvature of the matrix elements as a function of \vec{k} is positive, linear interpolation overestimates the matrix elements, while for negative curvature they are underestimated. Given the arrangement of tetrahedra as described in Sec. III, the errors cancel if the result is integrated over the entire reciprocal cell, as would be the case for insulators or completely filled bands in metals. However, in metals this cancellation is incomplete, because the integration region is only a fraction of the Brillouin zone, so that one curvature dominates.

The integration error is related to the mean curvature of the matrix elements. Using Green's theorem, it is possible to convert the volume integral of the second derivatives into a Fermi surface integral, which involves only first derivatives of the matrix elements. First derivatives can be obtained from the linearly interpolated matrix elements. The resulting expression allows us to include the effect of the curvature of the matrix elements without ever having to calculate second derivatives.

We first evaluate the integration error $\delta\langle X\rangle_T = \int_T d^3k [X(\vec{k}) - \bar{X}(\vec{k})]$ resulting from a single tetrahedron, indicated by the subscript T . In a second step we average the result over the unit cell and convert the volume integration into a surface integral. Note that the band indices are suppressed in this section.

We begin by comparing the integral of a general quadratic function

$$X(\vec{k}) = a + \sum_i b_i k_i + \frac{1}{2} \sum_{ij} k_i c_{ij} k_j \quad (8)$$

with that of the linearly interpolated function. Terms of higher than the quadratic order will not affect the leading-order estimate of the interpolation error.

The tetrahedron is defined by its four corners, one of which is, without restriction of generality, placed at the origin and the remaining three are at $t_i = (t_{1i}, t_{2i}, t_{3i})$ for $i = 1, 2, 3$. To simplify the discussion we transform the problem into a new coordinate system, with the new coordinates denoted by s_i ,

$$k_i = \sum_j t_{ij} s_j. \quad (9)$$

The matrix elements in the new coordinate system have the form

$$X(\vec{s}) = \bar{a} + \sum_i \bar{b}_i s_i + \frac{1}{2} \sum_{ij} s_i \bar{c}_{ij} s_j \quad (10)$$

with coefficients $\bar{a} = a$, $\bar{b}_i = \sum_j b_j t_{ji}$, and $\bar{c}_{ij} = \sum_{kl} t_{ki} c_{kl} t_{lj}$. In the new representation the tetrahedron occupies the space with $s_i \geq 0$ for $i = 1, 2, 3$ and $\sum_{i=1}^3 s_i \leq 1$.

The linearly interpolated matrix elements $\bar{X}(s)$ have the form

$$\bar{X}(\vec{s}) = \bar{a} + \sum_i (\bar{b}_i + \frac{1}{2} \bar{c}_{ii}) s_i. \quad (11)$$

The difference between the integrals of the two functions can be evaluated analytically.

$$\begin{aligned} \delta\langle X\rangle_T &= \det|t_{ij}| \int_T d^3s \frac{1}{2} \left[\sum_{ij} s_i \bar{c}_{ij} s_j - \sum_i \bar{c}_{ii} s_i \right] \\ &= \frac{1}{6} \det|t_{ij}| \frac{1}{40} \left[\sum_{i \neq j} \bar{c}_{ij} - 3 \sum_i \bar{c}_{ii} \right]. \end{aligned} \quad (12)$$

Now we replace the coefficients c_{ij} by the average second derivatives of the matrix elements. $\frac{1}{6} \det|t_{ij}|$ is simply the volume of the tetrahedron V_T , so that Eq. (12) can be expressed as

$$\delta\langle X\rangle_T = V_T \sum_{ij} \left\langle \frac{\partial^2 X}{\partial k_i \partial k_j} \right\rangle_T C_{ij} \Delta^2, \quad (13)$$

where $\Delta = \sqrt[3]{\det|t|}$ is the characteristic k point spacing and

$$C_{ij} = \frac{1}{40\Delta^2} \left[\sum_{l \neq m} t_{il} t_{jm} - 3 \sum_l t_{il} t_{jl} \right] \quad (14)$$

is a dimensionless form factor describing shape and orientation of the tetrahedron.

Summing the result for $\delta\langle X\rangle_T$ over all occupied tetrahedra and division by the cell volume yields a closed expression for the interpolation error of the expectation value:

$$\delta\langle X\rangle = \left\langle \sum_{ij} \frac{\partial^2 X}{\partial k_i \partial k_j} C_{ij} \right\rangle \Delta^2. \quad (15)$$

This clearly reveals the Δ^2 behavior of the interpolation error that is evident from Figs. 2, 3, and 4 for the conventional tetrahedron method.

In the following we apply the Gauss theorem to transform the expression for the integration error into an integral over the Fermi surface. For this purpose we replace the form factor by its average over all six types of tetrahedra. This step is exact in the leading order, because for the leading order the curvature of the matrix elements can be considered constant within an entire submesh cell, so that the integral factorizes. It is only permitted if each subcell is divided in the same way, as described in Sec. III. If the Brillouin-zone integral is performed only over the irreducible cell, as in most previous implementations of the tetrahedron method, the condition for this step is violated and, as a result, our correction formula would fail.

We obtain

$$\begin{aligned} \delta\langle X\rangle &= \frac{1}{V_G} \sum_{ij} \langle C_{ij} \rangle \int_{V_G} d^3k \frac{\partial^2 X}{\partial k_i \partial k_j} \Delta^2 \\ &= \frac{1}{V_G} \sum_{ij} \langle C_{ij} \rangle \oint_{\epsilon = \epsilon_F} d^2 A_i \frac{\partial X}{\partial k_j} \Delta^2, \end{aligned} \quad (16)$$

where the last integral is a surface integral over the Fermi surface.

Now we replace the average form factor by the form

factor of each contributing tetrahedron and obtain

$$\delta\langle X \rangle = \frac{1}{V_G} \sum_{ij} \oint_{\epsilon=\epsilon_F} d^2 A_i C_{ij} \frac{\partial X}{\partial k_j} \Delta^2. \quad (17)$$

We do the following substitutions:

$$\int d^2 A_i = \int d^2 |A| \frac{1}{|\nabla_k \epsilon|} \frac{\partial \epsilon}{\partial k_i}, \quad (18)$$

$$\sum_i \frac{\partial \epsilon}{\partial k_i} t_{ij} = \epsilon_{j+1} - \epsilon_1, \quad (19)$$

$$\sum_i \frac{\partial X}{\partial k_i} t_{ij} = X_{j+1} - X_1, \quad (20)$$

where the ϵ_i and X_i are the one-particle energies and matrix elements at the four corners of the tetrahedron. By inserting this into Eq. (17) we obtain, after some re-ordering,

$$\begin{aligned} \delta\langle X \rangle &= \sum_T D_T(\epsilon_F) \frac{1}{40} \left[\sum_{i \neq j} (X_{i+1} - X_1)(\epsilon_{j+1} - \epsilon_1) \right. \\ &\quad \left. - 3 \sum_i (X_{i+1} - X_1)(\epsilon_{i+1} - \epsilon_1) \right] \\ &= \sum_T D_T(\epsilon_F) \frac{1}{40} \sum_{i=1}^4 X_i \sum_{j=1}^4 (\epsilon_j - \epsilon_i). \end{aligned} \quad (21)$$

The corresponding correction dw_i to the integration weights has an extremely simple form:

$$dw_i = \frac{d\delta\langle X \rangle}{dX_i} = \sum_T \frac{1}{40} D_T(\epsilon_F) \sum_{j=1}^4 (\epsilon_j - \epsilon_i). \quad (22)$$

Only tetrahedra adjacent to \vec{k}_i contribute to the weight w_i .

The form factor for the tetrahedra provides a direct measure for the quality of a tetrahedron shape. Optimizing the tetrahedra for parabolic bands results in the criterion that the trace of the form factor $\sum_i C_{ii}$ should be minimized under the constraints imposed by the space-group symmetry. It is, however, our impression that the shape of the tetrahedra has only a minor effect on the accuracy of the result—except in pathological cases.

VI. DISCUSSION

In this section we discuss selected issues that are relevant to our findings in the light of the present work. This discussion is not meant as a review of previous work, nor does it aim at completeness.

A. Integration errors due to the approximation of the Fermi surface

So far we have only considered the errors due to integration in the bulk of the occupied states. Here we

shall analyze the errors due to the approximation of the Fermi surface by a polyhedron in the linear tetrahedron method.

We will first focus on a single triangular face of the polyhedron representing the Fermi surface, and the resulting expression will guide us in the following discussion of the integration error. We calculate the volume between the Fermi surface and the triangular face of the tetrahedron. Here we will choose the Fermi level of the true and that of the linearly interpolated bands to be the same. This is different from the common use of the tetrahedron method, where the total charge is constrained. The transformation from the constant-Fermi-level ensemble to a constant-particle ensemble will be done later. We perform an analysis analogous to that in Sec. V, with the main difference that here we deal with a two-dimensional integration and the matrix elements are replaced by the distance $k_F - \vec{k}_F$ between the true Fermi surface and the planar triangle. The excess electron number, which is directly related to this volume, is then given by

$$\delta N_{e1,T} = \frac{A_T}{V_G} \sum_{ij} \frac{\partial^2 k_F}{\partial k_i \partial k_j} C_{ij} \Delta^2, \quad (23)$$

where A_T is the area of the triangle and the summation runs over two dimensions. The form factor C_{ij} of the triangle is

$$C_{ij} = \frac{1}{24\Delta^2} \left[\sum_{l \neq m} t_{il} t_{jm} - 2 \sum_l t_{il} t_{jl} \right]. \quad (24)$$

t_{ij} are the two vectors that span the triangle. We again choose to define Δ as the mean grid spacing. The corresponding error in the expectation value of an operator X is obtained in the highest order in Δ by multiplying $\delta N_{e1,T}$ by the matrix element obtained somewhere on the triangle.

Let us now discuss the implication of this expression for the convergence behavior of the tetrahedron method. Given a fixed Fermi energy, the electron number is obviously in error by a number proportional to Δ^2 . Since the tetrahedron method adjusts the Fermi level until the electron number is correct, the Fermi level in the tetrahedron method converges as Δ^2 , but the electron number is exact. If the curvature of the Fermi surface were completely uniform, the integral of the matrix elements would be in error only because the integration region of order Δ^2 is displaced within a tetrahedron by a distance proportional to Δ , resulting in a total integration error proportional to Δ^3 .

In order to discuss the case of changing curvature, let us consider the extreme cases of Fermi surface sheets, one from a free-electron band and one from an inverted free-electron or hole band. Since the curvatures of the two bands are opposite, the Fermi level is unchanged, but the number of states in the electron band is underestimated and that in the other band is overestimated by a factor proportional to Δ^2 . This results in an integration error for the matrix elements of the same order, if the average values of the matrix elements at the two sheets of the Fermi surface differ. A similar effect also occurs in general bands. Hence, for general integrals the

tetrahedron method still converges as Δ^2 , owing to the approximation of the Fermi surface.

As mentioned before, this convergence behavior is not valid for the total energy or the band-structure energy, for which the Fermi surface approximation only leads to errors of order Δ^4 , because band-structure energy and total energy are variational with respect to a change in the Fermi surface.

B. Higher-order interpolation schemes

There are a number of possible extensions of the tetrahedron method. Very early, MacDonald *et al.*¹² suggested a very flexible approach, namely, the hybrid tetrahedron method. The general idea is to interpolate the energy bands and matrix elements by nonlinear functions such as piecewise quadratic interpolation, and then integrate the interpolated function using the standard tetrahedron method on a finer submesh. As the submesh for the tetrahedron method can be made arbitrarily fine without much computational overhead, the accuracy of the hybrid method is dominated by the first high-order interpolation. Hence, with the piecewise quadratic function the result of the direct quadratic tetrahedron method¹³ is recovered.

A more sophisticated interpolation based on a Fourier interpolation of the bands has also been suggested.^{14–16} This interpolation would be closer to the special-point method, which itself is usually justified by the rapid convergence of the Fourier-transformed bands and matrix elements.

As mentioned in Sec. II, all higher-order methods can be mapped onto a sampling formula, so that substantial savings in computational time and memory requirements can be obtained. A procedure that is valid for any hybrid method can be outlined as follows.

(1) A coarse grid for the higher-order interpolation is defined. The irreducible points can be found analogously to the procedure described in Sec. III. The irreducible k points on the coarse grid will be denoted as upper-case \vec{K}_j in the following. Similarly, one defines a fine grid for the tetrahedron integration of the interpolated function as described in Sec. III.

(2) The energy values $\epsilon(\vec{K}_j)$ for the irreducible k points on the coarse grid are obtained.

(3) The energy values $\tilde{\epsilon}(\vec{k}_i)$ on the fine mesh are obtained with the high-order interpolation.

(4) Using the corrected tetrahedron method described here, one calculates the integration weights w_{in} , corresponding to the bands given by $\tilde{\epsilon}(k)$, on the irreducible k points on the fine grid. For calculations of the density of states, the energy derivative of the integration weights for the integrated density of states is used.

(5) A set of functions $W_j(\vec{k})$ is defined such that $W_j(\vec{k})$ is unity at the irreducible point \vec{K}_j on the coarse grid, and vanishes for all other k points on the coarse grid. Using the high-order interpolation scheme, one obtains the values $W_j(\vec{k}_i)$ on the irreducible k points \vec{k}_i of the fine grid.

(6) The integration weights W_{jn} for the course grid are

given as

$$W_{jn} = \sum_{k_i} W_j(k_i) w_{in}. \quad (25)$$

(7) The matrix elements are calculated on the irreducible k points on the coarse grid and immediately added to the expectation value with the weights W_{jn} so that

$$\langle X \rangle = \sum_{K_j} X_n(K_j) W_{jn}. \quad (26)$$

C. Band crossings

Using high-order interpolation schemes increases the problems related to band crossings. In some instances it is difficult to decide from the values on a discrete grid alone how the bands are connected. Typically a band is identified by simply counting the number of states at each k point from the lowest eigenvalue. With this choice, it is implicitly assumed that all band crossings are avoided. A low-order interpolation, such as the linear tetrahedron method, limits the error to that tetrahedron in which the band crossing occurs. Higher-order interpolation on the other hand may result in artificial oscillations further away from the band crossing, and, in the worst case, may lead to an opening of artificial sheets of the Fermi surface. If such cases are important, one has to inspect the band structure and connect the bands “by hand.”

In the linear tetrahedron method errors are introduced only by those band crossings that occur right at the Fermi level. Integration weights at energy levels that lie sufficiently below the Fermi level have a value that is identical to the geometric weight, and are independent of the band index. Therefore they are independent of the way the bands are connected. Hence, we have to consider those lines or points where band crossings intersect with the Fermi level. At these lines and points errors of order Δ^3 and Δ^4 , respectively, are introduced in the linear tetrahedron method. It should be noted that this result is independent of whether the band crossing is accidental or due to a symmetry-required degeneracy. We have, however, excluded pathological cases, such as dispersionless, partially filled bands.

D. Broadening methods

In order to avoid the problems of the traditional tetrahedron method with plane-wave-based electronic-structure methods, broadening methods are commonly used.^{17–19} Broadening methods replace the density of states by a sum of smooth functions such as Gaussians, centered at the energy values of the irreducible k points. The motivation for such methods is the following. Given an infinitely fine grid, the weighted density of states can be obtained as a sum of δ functions centered at the energy eigenvalues and multiplied by their matrix elements. If the k space is discretized, the δ functions are smeared out

so that a smooth density of states is obtained and no discontinuities disrupt the self-consistency cycle. Most applications replace the δ functions by Gaussians of a given width, but other functions have also been used.¹⁹ De Vita and Gillan²⁰ have introduced a variant of the broadening methods, which is based on a finite-temperature calculation without broadening the density of states, followed by a correction that recovers the zero-temperature total energy up to order T^3 , where T is the temperature used in the calculation.

The similarity of the sampling formula obtained from the broadening methods and that from the tetrahedron method suggests a comparison of the two. What corresponds to the broadening functions is obtained as the energy derivative of the integration weights in the tetrahedron method. This function is shown in Fig. 7 for a simple cubic lattice and a linear band ascending in the [111] direction. The width of these functions scales with the steepness of the bands. Hence, if steep and flat bands are present, as in transition metals, the tetrahedron method leads to broadening functions with different widths at different irreducible k points or bands. This feature, which is not present in the broadening methods, results in a consistent description of energy bands with different shapes, namely, if steep and flat bands cross the Fermi surface.

Whereas the traditional tetrahedron method is variational with respect to changes of the Fermi surface, the total energy obtained with the broadening methods is not variational with respect to changes of the occupations. Thus the Hellmann-Feynman theorem is no longer directly applicable. When calculating forces for metals, an additional term that describes the reoccupation of states close to the Fermi surface must be considered. It should be noted, however, that our correction formula is also not strictly variational.²¹

The occupations obtained from the smearing meth-

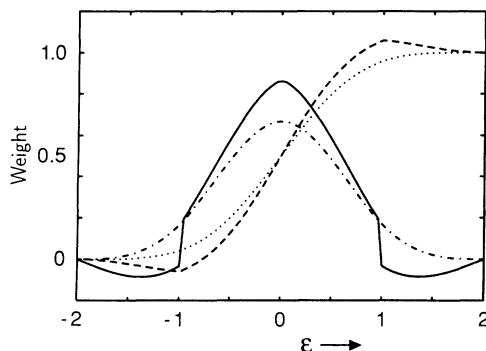


FIG. 7. Integration weights (dashed, with correction; dotted, without correction) for a single k point as a function of the Fermi energy and their energy derivatives (solid, with correction; dash-dotted, without correction) as obtained from the tetrahedron method. The energy derivative of the integration weights corresponds to the smearing function of the broadening methods (often Gaussians), which, in contrast to those obtained by the tetrahedron method, do not adjust their shape to the actual steepness and shape of the energy bands. Here we used a simple cubic k -space grid, and an energy band with a constant gradient along the [111] direction.

ods can, however, be obtained as the minimum of a different functional. Let us first define a notation: if the broadening function is g , then the occupation is $f_i = G(\epsilon_i - \epsilon_F) = \int_{-\infty}^{\epsilon_F} d\epsilon' g(\epsilon' - \epsilon_i)$. G^{-1} is the function inverse to the integrated broadening function G , so that $G^{-1}(G(\epsilon)) = \epsilon$. The functional that is minimized by the broadening methods has the form

$$F = E - \sum_{k_i} \int_0^{f_i} df' G^{-1}(f'), \quad (27)$$

where a free-energy-like term is added to the zero-temperature total energy. The variational principle of F with respect to variations in the occupations under the constraint of a constant electron number yields exactly the occupation numbers predicted by the broadening methods. If the contributions from reoccupying states at the Fermi surface are neglected while calculating forces, one obtains exactly the gradient of the functional F , but not that of the original functional E .

It has been argued that one advantage of the broadening methods is that they produce a smooth density of states, whereas the tetrahedron method shows typical Gauss oscillations. However, a smooth density of states can also be obtained from the tetrahedron method simply by broadening the result. This approach has been frequently used for density-of-states plots, if the number of k points was insufficient. We do not recommend the use of a broadening function for the density of states in total energy calculations using the tetrahedron method because, as in the broadening methods, it destroys the variational principle. Furthermore, the oscillatory behavior produced by the tetrahedron method occurs close to van Hove singularities, where the broadening methods break down: at band edges, for example, the smooth density of states comes at the expense of a broadening of the band itself.

APPENDIX A: NUMBER OF STATES

Here we list the expressions for the integrated density-of-states or number-of-states function $n(\epsilon)$ from a given tetrahedron. The number-of-states function is used to determine the Fermi level. The expressions shown are similar to those given in previous papers.^{1,2} For the sake of simplicity we have omitted all band indices. The one-particle energies at the corners of the tetrahedron are $\epsilon_1, \epsilon_2, \epsilon_3, \epsilon_4$, which are ordered according to increasing values. ϵ_{ij} is a shorthand notation for $\epsilon_i - \epsilon_j$. V_T is the reciprocal-space volume of the tetrahedron, and V_G is the volume of the reciprocal unit cell.

$$n(\epsilon) = 0 \quad (A1)$$

for $\epsilon < \epsilon_1$,

$$n(\epsilon) = \frac{V_T (\epsilon - \epsilon_1)^3}{V_G \epsilon_{21} \epsilon_{31} \epsilon_{41}} \quad (A2)$$

for $\epsilon_1 < \epsilon < \epsilon_2$,

$$n(\epsilon) = \frac{V_T}{V_G} \frac{1}{\epsilon_{31}\epsilon_{41}} \left[\epsilon_{21}^2 + 3\epsilon_{21}(\epsilon - \epsilon_2) + 3(\epsilon - \epsilon_2)^2 - \frac{\epsilon_{31} + \epsilon_{42}}{\epsilon_{32}\epsilon_{42}} (\epsilon - \epsilon_2)^3 \right] \quad (\text{A3})$$

for $\epsilon_2 < \epsilon < \epsilon_3$,

$$n(\epsilon) = \frac{V_T}{V_G} \left(1 - \frac{(\epsilon_4 - \epsilon)^3}{\epsilon_{41}\epsilon_{42}\epsilon_{43}} \right) \quad (\text{A4})$$

for $\epsilon_3 < \epsilon < \epsilon_4$, and

$$n(\epsilon) = \frac{V_T}{V_G} \quad (\text{A5})$$

for $\epsilon > \epsilon_4$.

APPENDIX B: INTEGRATION WEIGHTS

Here we give the expressions that result in the integration weights w_{nj} . By w_1, w_2, w_3 , and w_4 we denote the contribution to the integration weights at the four corners of a tetrahedron, which are again ordered according to increasing one-particle energies. Note that the band index n is suppressed.

For a fully unoccupied tetrahedron, i.e., $\epsilon_F < \epsilon_1$, the contributions vanish:

$$w_1 = w_2 = w_3 = w_4 = 0. \quad (\text{B1})$$

For $\epsilon_1 < \epsilon_F < \epsilon_2$, we obtain

$$w_1 = C \left[4 - (\epsilon_F - \epsilon_1) \left(\frac{1}{\epsilon_{21}} + \frac{1}{\epsilon_{31}} + \frac{1}{\epsilon_{41}} \right) \right], \quad (\text{B2})$$

$$w_2 = C \frac{\epsilon_F - \epsilon_1}{\epsilon_{21}}, \quad (\text{B3})$$

$$w_3 = C \frac{\epsilon_F - \epsilon_1}{\epsilon_{31}}, \quad (\text{B4})$$

$$w_4 = C \frac{\epsilon_F - \epsilon_1}{\epsilon_{41}} \quad (\text{B5})$$

with

$$C = \frac{V_T}{4V_G} \frac{(\epsilon_F - \epsilon_1)^3}{\epsilon_{21}\epsilon_{31}\epsilon_{41}}. \quad (\text{B6})$$

For $\epsilon_2 < \epsilon_F < \epsilon_3$, we obtain

$$w_1 = C_1 + (C_1 + C_2) \frac{\epsilon_3 - \epsilon_F}{\epsilon_{31}} + (C_1 + C_2 + C_3) \frac{\epsilon_4 - \epsilon_F}{\epsilon_{41}}, \quad (\text{B7})$$

$$w_2 = C_1 + C_2 + C_3 + (C_2 + C_3) \frac{\epsilon_3 - \epsilon_F}{\epsilon_{32}} + C_3 \frac{\epsilon_4 - \epsilon_F}{\epsilon_{42}}, \quad (\text{B8})$$

$$w_3 = (C_1 + C_2) \frac{\epsilon_F - \epsilon_1}{\epsilon_{31}} + (C_2 + C_3) \frac{\epsilon_F - \epsilon_2}{\epsilon_{32}}, \quad (\text{B9})$$

$$w_4 = (C_1 + C_2 + C_3) \frac{\epsilon_F - \epsilon_1}{\epsilon_{41}} + C_3 \frac{\epsilon_F - \epsilon_2}{\epsilon_{42}}, \quad (\text{B10})$$

with

$$C_1 = \frac{V_T}{4V_G} \frac{(\epsilon_F - \epsilon_1)^2}{\epsilon_{41}\epsilon_{31}}, \quad (\text{B11})$$

$$C_2 = \frac{V_T}{4V_G} \frac{(\epsilon_F - \epsilon_1)(\epsilon_F - \epsilon_2)(\epsilon_3 - \epsilon_F)}{\epsilon_{41}\epsilon_{32}\epsilon_{31}}, \quad (\text{B12})$$

$$C_3 = \frac{V_T}{4V_G} \frac{(\epsilon_F - \epsilon_2)^2(\epsilon_4 - \epsilon_F)}{\epsilon_{42}\epsilon_{32}\epsilon_{41}}. \quad (\text{B13})$$

For $\epsilon_3 < \epsilon_F < \epsilon_4$, the weights are

$$w_1 = \frac{V_T}{4V_G} - C \frac{\epsilon_4 - \epsilon_F}{\epsilon_{41}}, \quad (\text{B14})$$

$$w_2 = \frac{V_T}{4V_G} - C \frac{\epsilon_4 - \epsilon_F}{\epsilon_{42}}, \quad (\text{B15})$$

$$w_3 = \frac{V_T}{4V_G} - C \frac{\epsilon_4 - \epsilon_F}{\epsilon_{43}}, \quad (\text{B16})$$

$$w_4 = \frac{V_T}{4V_G} - C \left[4 - \left(\frac{1}{\epsilon_{41}} + \frac{1}{\epsilon_{42}} + \frac{1}{\epsilon_{43}} \right) (\epsilon_4 - \epsilon_F) \right], \quad (\text{B17})$$

with

$$C = \frac{V_T}{4V_G} \frac{(\epsilon_4 - \epsilon_F)^3}{\epsilon_{41}\epsilon_{42}\epsilon_{43}}. \quad (\text{B18})$$

For a fully occupied tetrahedron the contribution for each corner is identical:

$$w_1 = w_2 = w_3 = w_4 = \frac{V_T}{4V_G}. \quad (\text{B19})$$

The correction formula, described in this paper, is found in Eq. (22) and should be added to these uncorrected weights. All other symbols are explained in Appendix A.

APPENDIX C: DENSITY OF STATES

The contribution of one tetrahedron to the density of states at energy ϵ is given by

$$D_T(\epsilon) = 0 \quad (\text{C1})$$

for $\epsilon < \epsilon_1$ and for $\epsilon_4 < \epsilon$,

$$D_T(\epsilon) = \frac{V_T}{V_G} \frac{3(\epsilon - \epsilon_1)^2}{\epsilon_{21}\epsilon_{31}\epsilon_{41}} \quad (\text{C2})$$

for $\epsilon_1 < \epsilon < \epsilon_2$,

$$D_T(\epsilon) = \frac{V_T}{V_G} \frac{1}{\epsilon_{31}\epsilon_{41}} \left[3\epsilon_{21} + 6(\epsilon - \epsilon_2) - 3 \frac{(\epsilon_{31} + \epsilon_{42})(\epsilon - \epsilon_2)^2}{\epsilon_{32}\epsilon_{42}} \right] \quad (\text{C3})$$

for $\epsilon_2 < \epsilon < \epsilon_3$, and

$$D_T(\epsilon) = \frac{V_T}{V_G} \frac{3(\epsilon_4 - \epsilon)^2}{\epsilon_{41}\epsilon_{42}\epsilon_{43}} \quad (\text{C4})$$

for $\epsilon_3 < \epsilon < \epsilon_4$.

Symbols are explained in Appendix A.

* Part of this work was performed while the author was at Max-Planck-Institut FKF, Stuttgart, Germany.

¹ O. Jepsen and O.K. Andersen, *Solid State Commun.* **9**, 1763 (1971).

² G. Lehmann and M. Taut, *Phys. Status Solidi B* **54**, 469 (1972).

³ A. Baldereschi, *Phys. Rev. B* **7**, 5212 (1973).

⁴ D.J. Chadi and M.L. Cohen, *Phys. Rev. B* **8**, 5747 (1973).

⁵ H.J. Monkhorst and J.D. Pack, *Phys. Rev. B* **13**, 5188 (1976).

⁶ O. Jepsen and O.K. Andersen, *Phys. Rev. B* **29**, 5965 (1984).

⁷ L. Kleinman, *Phys. Rev. B* **28**, 1139 (1983).

⁸ P.E. Blöchl, Ph.D. thesis, University of Stuttgart, Germany, 1989.

⁹ G.P. Das, P. Blöchl, O.K. Andersen, N.E. Christensen, and O. Gunnarsson, *Phys. Rev. Lett.* **63**, 1168 (1989); O.K. Andersen, A.I. Liechtenstein, C.O. Rodriguez, I.I. Mazin, O. Jepsen, V.P. Antropov, O. Gunnarsson, and S. Gopalan, *Physica C* **185-189**, 147 (1991); G.H.O. Daalderop, P.J. Kelly, and F.J.A. den Broeder, *Phys. Rev. Lett.* **68**, 682 (1992); M. van Schilfgaarde and F. Herman, *ibid.* **71**, 1923 (1993).

¹⁰ W.M. Temmerman, P.A. Sterne, F.Y. Guo, and Z. Szotek, *Mol. Simul.* **4**, 153 (1989).

¹¹ C.J. Bradley and A.P. Cracknell, *The Mathematical Theory of Symmetry in Solids* (Clarendon, Oxford, 1972).

¹² A.H. MacDonald, S. Vosko, and P.T. Coleridge, *J. Phys. C* **12**, 2991 (1979).

¹³ M.S. Methfessel, M.H. Boon, and F.M. Mueller, *J. Phys. C* **16**, L949 (1983).

¹⁴ D.G. Shankland, in *Computational Methods in Band Theory*, edited by P. Marcus, J. Janak, and A. Williams (Plenum, New York, 1971), p. 362.

¹⁵ D.D. Koelling and J.H. Wood, *J. Comput. Phys.* **67**, 253 (1986).

¹⁶ W.E. Pickett, H. Krakauer, and P.B. Allen, *Phys. Rev. B* **38**, 2721 (1988).

¹⁷ K.-M. Ho, C.-L. Fu, B.N. Harmon, W. Weber, and D.R. Hamann, *Phys. Rev. Lett.* **49**, 673 (1982); C.-L. Fu and K.-M. Ho, *Phys. Rev. B* **28**, 5480 (1983).

¹⁸ R.J. Needs, R.M. Martin, and O.H. Nielsen, *Phys. Rev. B* **33**, 3778 (1986).

¹⁹ M. Methfessel and A.T. Paxton, *Phys. Rev. B* **40**, 3616 (1989).

²⁰ A. De Vita and M.J. Gillan, *J. Phys. Condens. Matter* **3**, 6225 (1991).

²¹ In principle it is also possible to determine variationally the Fermi surface in the corrected tetrahedron method. One introduces a fictitious energy surface, which is used, like the true one-particle energies before, to determine the integration weights. This fictitious energy surface is then adjusted, until the band-structure energy, as obtained from our sampling formula with the true one-particle energies and the weights obtained from the fictitious energies, is minimized. During the minimization the constraint of constant particle number must be imposed.

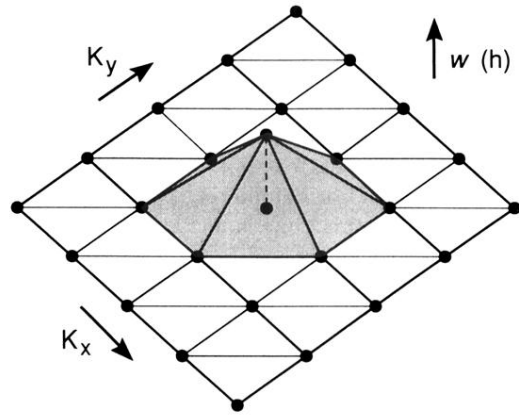


FIG. 6. Two-dimensional, schematic illustration of the functions $w_j(\vec{k})$ that result in the integration weights when integrated.